High-Performance Hydrogen-Selective Pd-Ag Membranes Modified with Pd-Pt Nanoparticles for Use in Steam Reforming Membrane Reactors

Iliya Petriev *, Polina Pushankina , Georgy Andreev , Stepan Dzhimak

Posted Date: 21 November 2023

doi: 10.20944/preprints202311.1260.v1

Keywords: hydrogen permeability; Pd-membranes; nanostars; hollow nanoparticles; modified surface; water gas shift reaction; membrane reactors

Article

High-Performance Hydrogen-Selective Pd-Ag Membranes Modified with Pd-Pt Nanoparticles for Use in Steam Reforming Membrane Reactors

Iliya Petriev [1,2,*], Polina Pushankina [1], Georgy Andreev [1] and Stepan Dzhimak [1,2]

[1] Department of Physics, Kuban State University, Krasnodar 350040, Russia
[2] Laboratory of Problems of Stable Isotope Spreading in Living Systems, Southern Scientific Centre of the RAS, Rostov-on-Don 344006, Russia
* Correspondence: petriev_iliya@mail.ru

Abstract: A unique method for synthesizing a surface modifier for metallic hydrogen permeable membranes based on non-classic bimetallic pentagonally structured Pd-Pt nanoparticles has been developed. It was found that nanoparticles had unique hollow structure. This significantly reduces the cost of their production due to economical use of metal. According to the results of electrochemical studies, synthesized bimetallic Pd-Pt/Pd-Ag modifier showed excellent catalytic activity (up to 60.72 mA cm^{-2}), long-term stability and resistance to CO_{ads} poisoning in alkaline oxidation reaction of methanol. The membrane with pentagonally structured Pd-Pt/Pd-Ag modifier showed the highest hydrogen permeation flux density up to 27.3 mmol s^{-1} m^{-2}. Obtained hydrogen flux density were 2 times higher than that for membranes with classic Pd_{black}/Pd-Ag modifier and an order of magnitude higher than that for unmodified membrane. Since the rate of transcrystalline hydrogen transfer through a membrane increased, while the speed of transfer through defects remained unchanged, a one and a half times rise in selectivity of the developed Pd-Pt/Pd-Ag membranes was recorded and it amounted to 3514. Achieved results are due to both the synergistic effect of the combination of Pd and Pt metals in the modifier composition and the large number of available catalytically active centers, which are present as a result of non-classic morphology with high-index facets. The specific faceting, defect structure and unusual properties provide great opportunities for the application of nanoparticles in the areas of membrane reactors, electrocatalysis, petrochemical and hydrogen industries.

Keywords: hydrogen permeability; Pd-membranes; nanostars; hollow nanoparticles; modified surface; water gas shift reaction; membrane reactors

1. Introduction

The rapid development of the global economy is creating high demand for energy in almost all areas of industry [1–4]. However, the main source of energy today is still fossil fuels, the reserves of which are very limited [5–8]. A promising next-generation alternative energy source is hydrogen [9–12]. The key step between production and application of hydrogen is its separation and purification [13]. The membrane separation method is widely used in many areas, including hydrogen energy, due to its simplicity, low cost, high energy efficiency and environmental friendliness [14–17]. The need to design and produce membrane filters with increased hydrogen permeability and durability has formed an interest in exploring different materials with the best performance and hydrogen resistance.

Palladium-based membranes are the most demanded due to their unique hydrogen selectivity [18–21]. Nevertheless, the use of pure palladium in reactions involving hydrogen leads to poisoning and rapid mechanical destruction as a result of its embrittlement [22,23]. The solution would be to alloy palladium with other metals such as Ag, Cu, Ru, Au [24–26]. The addition of silver to the alloy improves mechanical resistance of palladium-based membranes and provides optimal hydrogen permeability. In their work [27], A. Suzuki et al. analyzed the inverse temperature dependence of hydrogen permeability through membranes made of pure Pd and its alloys. It was found that the addition of Ag to Pd increased hydrogen solubility at high temperature and suppressed the $\alpha \rightarrow \alpha'$

 doi:10.20944/preprints202311.1260.v1

phase transition. This provided a moderate increase in PCT factor at higher temperature and resulted in a continuous hydrogen permeability peak at higher peak temperature. Q. Zhou et al. [28] studied selectivity and permeability of membranes for hydrogen on the basis of binary Pd-Au and ternary Pd-Au-Ag alloys. According to their results, both an improvement in selectivity and a significant increase in hydrogen permeability up to 2.09×10^{-1} mol s^{-1} m^{-2} Pa^{-1} at 300 K are achieved when Ag is introduced in comparison with the Pd-Au alloy membrane.

Nevertheless, the problem of low and unstable permeability of palladium-containing membranes at low-temperature operation modes, where hydrogen transport is limited by surface processes, remains unsolved [29,30]. This is caused by an impure or an inactive metal membrane surface. Consequently, there is a kinetic inhibition of reaching balance between molecular hydrogen in the gas phase and atomic absorbed one in the palladium phase at the metal-hydrogen system border [31]. This condition can be partially overcome by surface activation. Thus, N. Vicinanza et al. [32] studied the effect of three-stage heat treatment of Pd77%Ag23% membranes in air on their hydrogen permeability. It was found that hydrogen permeability of membranes increased after each stage, as the use of air heat treatment technique directly affected the increase in the effective surface area of the membrane. Another way to activate the membrane surface is its modification with powdered catalytically active particles [33–36]. The most promising way is the application of nanoparticles, which have become widespread in many areas of science and industry due to unusual physical and chemical properties of nanoparticles [37–42]. Application of a nanoparticle-based modifying layer significantly increases a working surface area of a membrane, thereby promoting a chemisorption centers increase [43]. Platinum group metals can be such hydrogen chemisorbing powders.

Palladium and platinum are universal catalysts for many reactions and processes in hydrogen energy [44–47]. However, most reactions show structural sensitivity, i.e., activity and selectivity depend on controlling metal nanoparticles' shape and size and the arrangement of atoms on a surface [48–51]. Thus, the addition of high-index facets to palladium-based nanoparticles enhances their catalytic activity toward reactions involving hydrogen [52,53]. Therefore, pentagonally structured nanoparticles with a big number of high-energy facets are of major interest. Application of a modifier based on such nanoparticles to a surface of a palladium-containing membrane can significantly increase catalytic activity of the material and hydrogen permeability in low-temperature operation mode [54]. Consequently, the aim of this work was to study the effect of morphology and structure of bimetallic nanoparticles as a part of palladium-silver membrane modifiers on low-temperature membrane processes of deep hydrogen purification.

2. Results and Discussion

2.1. Morphology, structure features and preparation of nanoparticles on Pd basis

Classic monometallic palladium nanoparticles were also obtained in the study. Microphotographs of the synthesized particles as a part of the modifier are presented in Figure 1. The obtained particles had classic energetically favorable spherical shape. The average size for the 75% of particles was about 80-110 nm. This classic particle type was deliberately obtained for further comparison with developed pentatwinned nanoparticles in catalytic and membrane applications.

Preprints (www.preprints.org) | NOT PEER-REVIEWED | Posted: 21 November 2023 doi:10.20944/preprints202311.1260.v1

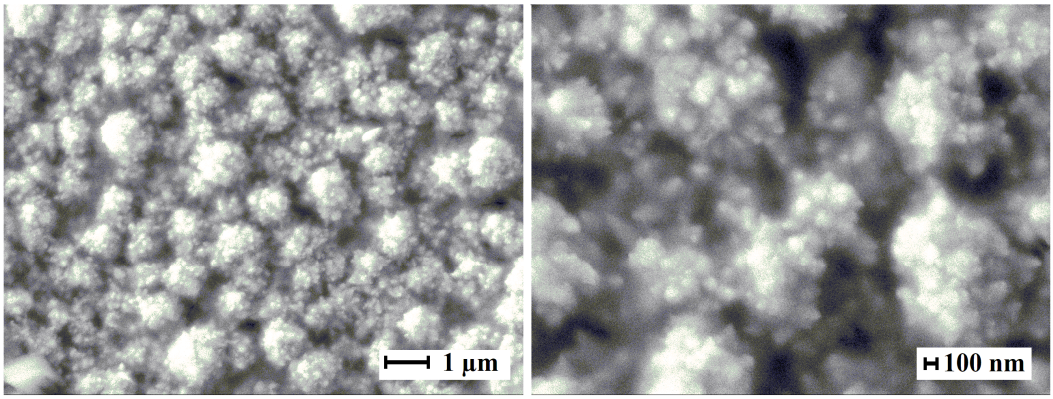

Figure 1. SEM images of classic palladium nanoparticles at different magnifications.

Non-classic bimetallic Pd-Pt nanoparticles as a part of the modifier with a fifth-order symmetry axis, which is unattainable in volumetric single crystals, were obtained in this study. The research concentrates on particle shaping and the combination of metals in their composition. The interest stems from the fact, that catalytic reactions can occur more selectively on certain facets or due to the introduction of a secondary metal that alters reactivity. Palladium and platinum are relatively similar in many basic characteristics. Both metals have face-centered cubic lattice with negligible difference in lattice parameter (Pd = 3890 Å, Pt = 3920 Å) and close standard reduction potentials. According to the density functional theory, platinum atoms occupy central positions, while palladium atoms concentrate on a surface during particle formation [55]. This can be explained by higher surface energy and cohesion energy of platinum atoms.

Nevertheless, in the synthesis of nanoparticles, their deliberate design considering faceted structure, homogeneity and compositional control remains a challenge, especially for nanoparticles, that are composed of catalytically favorable metal pairs. Therefore, a number of synthesis methods, which allow controlling the shape and composition of nanoparticles, have been developed in recent years [56]. The simplest and the most efficient method used in this work was the electrolytic deposition method. This method is unique because it provides additional control tools (voltage, current) along with classic tools for adjusting the shape and structure of particles (composition of the working solution, synthesis time). The developed method for the synthesis of non-classic pentatwinned particles combined several main distinctive features in comparison with the classic technique, which allowed to achieve similar particle morphology. Firstly, a two-step current variation was applied in the deposition process. At the beginning, sufficiently small current of 0.003 mA cm^{-2} was applied for a short period of time to promote the nucleation process. Such step is important in the synthesis process, as it is the nucleation shape, which underlies the nanoparticle, that can dictate self-assembly into larger architectures with new properties. Further, current was significantly increased and maintained until the end of the synthesis This allowed to carry out directed growth of specific facets of the particle surface and to give them a certain shape. Secondly, the surfactant and halide ions were used as tools for adjusting and controlling morphology. Properly selected surfactant concentration prevents particles from rounding during growth, preserving the inoculum geometry. Chloride in the working solution promotes oxidative etching, while bromide is responsible for selective passivation, stimulating the growth of facets with high Miller index. High-index facets exhibit much higher reactivity than low-index ones, because they have higher density of undercoordinated atoms located on steps and bends. These atoms have high reactivity, which is required for high catalytic activity.

Bimetallic Pd-Pt nanoparticles, synthesized in this work, had fifth-order rotational symmetry. Such symmetry can be observed in flowers of many plants, however, it is not typical for objects of non-living nature. Microphotographs of the surface of the obtained nanoparticles are shown in Figure 2. The particles had five-pointed star shape with high-energy facets with a big number of undercoordinated atoms. The average size for 60% of particles was in the range of 90-125 nm.

 doi:10.20944/preprints202311.1260.v1

According to EDS analysis, the resulting bimetallic modifier contained 94.8% of palladium and 5.2% of platinum.

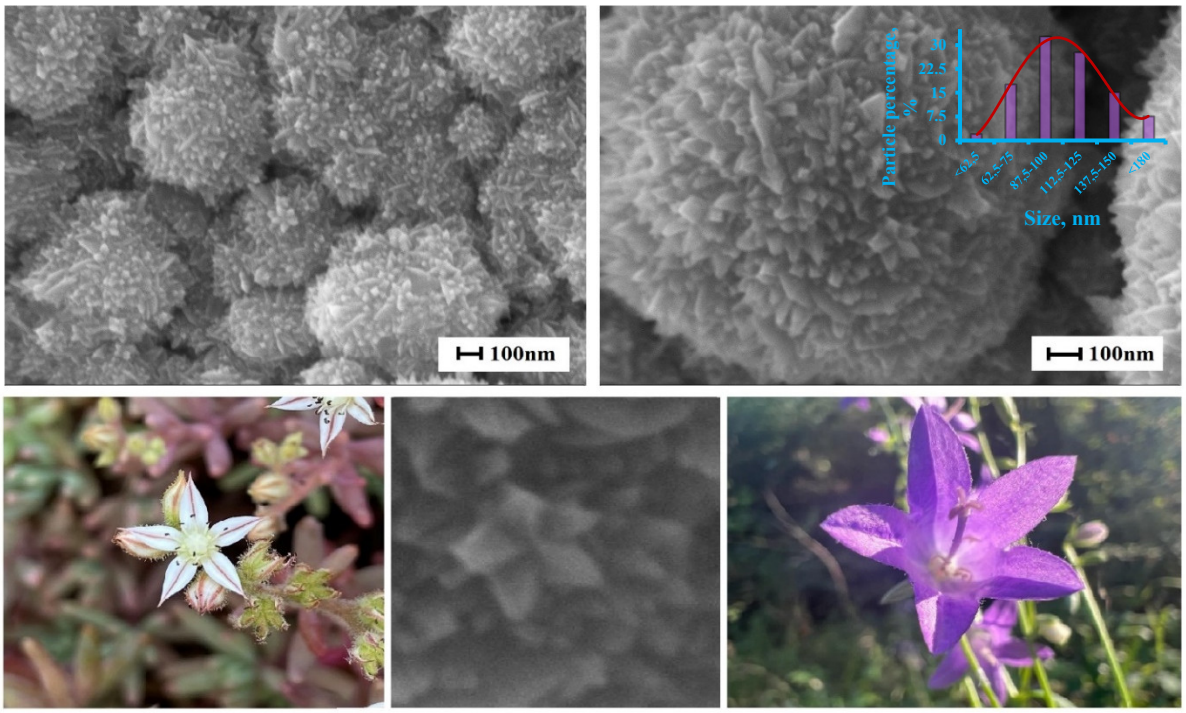

Figure 2. SEM images of bimetallic Pd-Pt nanoparticles.

Moreover, it was found, that pentagonal particles within the modifier were hollow. The obtained samples were weighed after the modifier was synthesized. However, according to the weighing results, the mass of the samples increased insignificantly. This raised a number of questions about the structure of the nanoparticles in the modifier composition. Chemical etching was used to determine structural features of the particle, as mechanical influence on particles of such a small size was a non-trivial task. During the etching process, the particle shell thinned and multiple explosion-like ruptures appeared. It was confirmed with electron microscopy (Figure 3). Etching was performed with hydrochloric acid according to the mechanism, which was described in the paper [57] for decahedral and icosahedral particles. This made it possible to speak about a similar destruction mechanism. The centers of destruction of pentagonal particles were the points of intersection of twin boundaries and disclinations on a particle surface. In other words, these were the points of maximum concentration of internal elastic stresses. Consequently, it can be assumed, that disclination content in electrolytically synthesized particles can lead to a formation of internal voids in them. This particle structure certainly has an economic benefit in terms of precious metal reduced consumption.

Preprints (www.preprints.org) | NOT PEER-REVIEWED | Posted: 21 November 2023 doi:10.20944/preprints202311.1260.v1

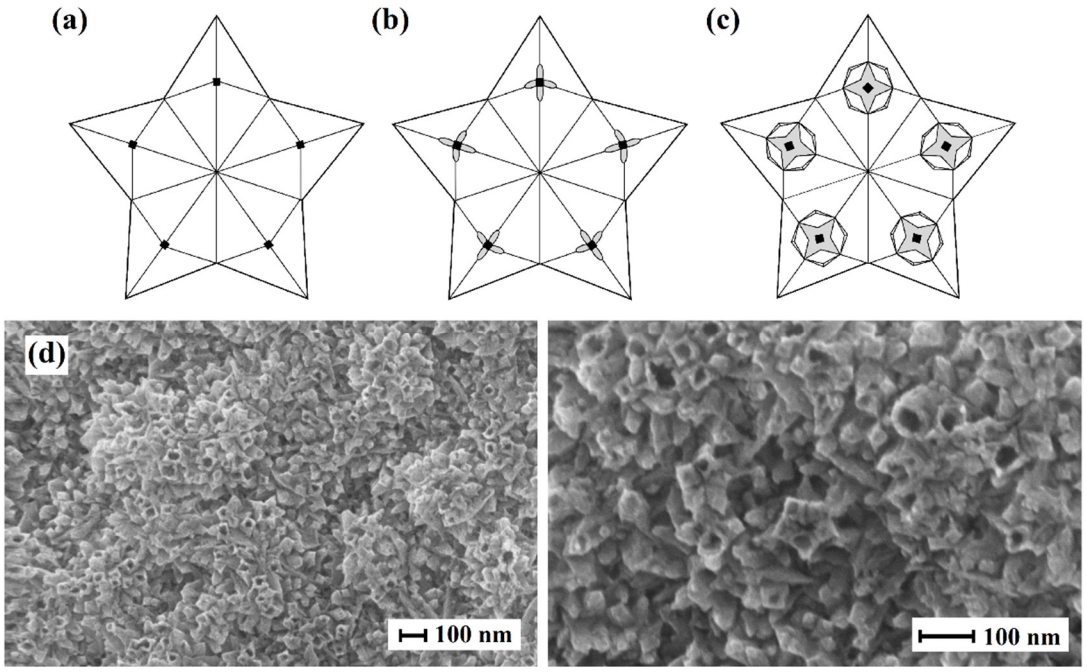

Figure 3. Scheme of crack formation in pentagonally structured nanoparticles during etching: (a) initial state of particles with disclination lines marked with dots; (b) formation of separate cracks at twin boundaries; (c) merging of cracks into a single star-shaped one. (d) SEM images of hollow Pd-Pt nanoparticles.

2.2. Catalytic characteristics of the bimetallic Pd-Pt modifier on pentatwinned nanoparticles basis

Electrochemical measurements of the obtained bimetallic pentagonally structured Pd-Pt/Pd-Ag modifier were carried out with cyclic voltammetry in alkaline methanol solution to assess catalytic properties. They were also compared with measurements for classic Pd_{black}/Pd-Ag modifier and unmodified electrode. Scanning was performed at potentials from –0.9 V to 0.5 V towards Ag/AgCl (saturated KCl) at a scan speed of 50 mV s^{-1} at room temperature. Measurements for each sample were made for one hundred cycles. The 30th cycles, which are the highest ones, are shown in Figure 4a. All the studied samples showed similar trends, namely a high current density peak around –0.1 V at anodic sweep (I_f), which is caused by oxidation of methanol. In addition, another peak around – 0.4 V at cathodic sweep (I_b) was observed for all samples, related to the accumulation of residual carbonaceous particles, which were produced during anodic sweep. However, forward peak current density and reverse peak current density for the electrode with bimetallic pentagonally structured Pd-Pt/Pd-Ag modifier were the highest and were approximately 60.72 mA cm^{-2} and 5.89 mA cm^{-2}, respectively. Achieved values were 3 times higher than those for the electrode with classic Pd_{black}/Pd-Ag modifier, 19.28 mA cm^{-2} and 3.37 mA cm^{-2} respectively, and more than two order of magnitude higher in comparison with unmodified electrode. The observed improvement in characteristics of pentagonally structured Pd-Pt/Pd-Ag modifier in methanol oxidation reaction can be explained with a bifunctional mechanism [58–60].

The process of methanol electrooxidation with electrodes modified with Pd-Pt particles can be described with the following stages [61]:

$$PdPt + CH_3OH \rightarrow PdPt\text{-}CO_{ads} + 4H^+ + 4e^- \quad (1)$$

$$PdPt + H_2O \rightarrow PdPt\text{-}OH_{ads} + H^+ + e^- \quad (2)$$

$$PdPt\text{-}CO_{ads} + PdPt\text{-}OH_{ads} \rightarrow CO_2 + 2PdPt + H^+ + e^- \quad (3)$$

According to (1), intermediate carbon monoxide forms (CO) are produced during methanol oxidation reaction and then further adsorbed on the surface of the Pd-Pt modifier ($PdPt\text{-}CO_{ads}$). The emerged CO_{ads} blocks the surface of the Pd-Pt modifier, thereby inhibiting the continuous oxidation

 doi:10.20944/preprints202311.1260.v1

process of methanol. PdPt-CO_{ads} can be oxidized by hydroxyl group (OH) with carbon dioxide (CO_2) formation.

In the synthesized bimetallic modifier, platinum is responsible for chemisorption of methanol and palladium is responsible for oxidation of water particles. Platinum adsorbs carbon intermediate compounds such as CO_{ads} and palladium adsorbs its counter intermediate compounds such as OH_{ads}, i.e., it catalyzes the dehydrogenation of water molecules. In the bimetallic PdPt modifier, the d-zone centers of platinum shift downwards and the Pt-CO_{ads} bond becomes weaker. At the same time, Pd-OH_{ads} reacts with it and eventually leads to a formation of CO_2. The reaction between Pt-CO_{ads} and Pd-OH_{ads} leads to a removal of strongly adsorbed CO_{ads} particles on active centers. The strong bonding between Pd-Pt atoms can also reduce the coordination between the Pt and –CO_{ads} bonds, thereby destroying the Pt-CO_{ads}. These synergistic effects significantly improve the overall characteristics of the Pd-Pt/Pd-Ag modifier. The enhanced electrocatalytic performance of pentagonally structured Pd-Pt/Pd-Ag modifier in methanol oxidation reaction can also be explained with high density of atomic steps, protrusions and fractures on high-index facets.

The resistance of catalytic coatings to CO_{ads} poisoning is usually assessed via the ratio of forward (I_f) to reverse (I_b) current density peaks [62]. In comparison with classic Pd_{black}/Pd-Ag modifier (5.7), pentagonally structured Pd-Pt/Pd-Ag one showed higher values of I_f/I_b ratio – 10.3. This indicates that poisoning particles are removed from the catalyst surface more efficiently and that the mutual contribution of palladium and platinum can significantly reduce CO poisoning during the reaction. The high value of the I_f/I_b ratio implies that most of the intermediate carbonaceous particles CO_{ads} are oxidized to CO_2 in the direct scan due to the presence of OH_{ads}.

Chronoamperometric tests of pentagonally structured Pd-Pt/Pd-Ag modifier, classic Pd_{black}/Pd-Ag modifier and unmodified electrode were carried out to study electrocatalytic stability, durability and resistance to methanol oxidation at fixed temperature. At the initial stage, modified electrodes had high current values, which can be explained by a big number of active centers on the surface. Typically, methanol is continuously oxidized on the surface of the modifier at a fixed potential, and many intermediate adsorbed CO_{ads} particles also begin to accumulate on the surface during methanol oxidation reaction. As can be seen from Figure 4b, the initial current of pentagonally structured Pd-Pt/Pd-Ag modifier was significantly higher than that of classic Pd_{black}/Pd-Ag modifier and unmodified electrode. This is an indicator of a higher charging of the double layer [63]. However, a rapid drop of current up to 500 s was observed due to the formation of CO-like intermediates, which were adsorbed on the active centers of catalysts. This prevented further oxidation of methanol [64]. It was recorded, that pentagonally structured Pd-Pt/Pd-Ag modifier demonstrated significantly higher current than classic Pd_{black}/Pd-Ag modifier and unmodified electrode over the entire time period, even though current drop was observed. Final current density of pentagonally structured Pd-Pt/Pd-Ag modifier was about 2.39 mA cm^{-2}, which was higher than that of classic Pd_{black}/Pd-Ag modifier (1.25 mA cm^{-2}) and unmodified electrode (0.01 mA cm^{-2}). In addition, pentagonally structured Pd-Pt/Pd-Ag modifier had the lowest calculated current density reduction (41 %) in comparison with classic Pd_{black}/Pd-Ag modifier (62 %). This indicated better resistance of Pd-Pt/Pd-Ag to poisoning in methanol oxidation reaction. The gradual decrease in current over time was an indicator of the good anti-poisoning ability of the modifier [63]. The slower current decline, which was observed for the electrode with pentagonally structured Pd-Pt/Pd-Ag modifier, indicated less accumulation of adsorbed CO_{ads} particles on the modifier surface. Therefore, it means that pentagonally structured Pd-Pt/Pd-Pd-Ag modifier showed superior electrocatalytic performance and better stability than classic Pd_{black}/Pd-Ag modifier and unmodified electrode towards alkaline oxidation reaction of methanol. The activity level in chronoamperometric measurements corresponded directly to the activity level in cyclic voltammetry measurements. The obtained results can be due to the synergistic effect of the palladium-platinum alloy, which has superior poisoning resistance in comparison with monometallic palladium.

Preprints (www.preprints.org) | NOT PEER-REVIEWED | Posted: 21 November 2023 doi:10.20944/preprints202311.1260.v1

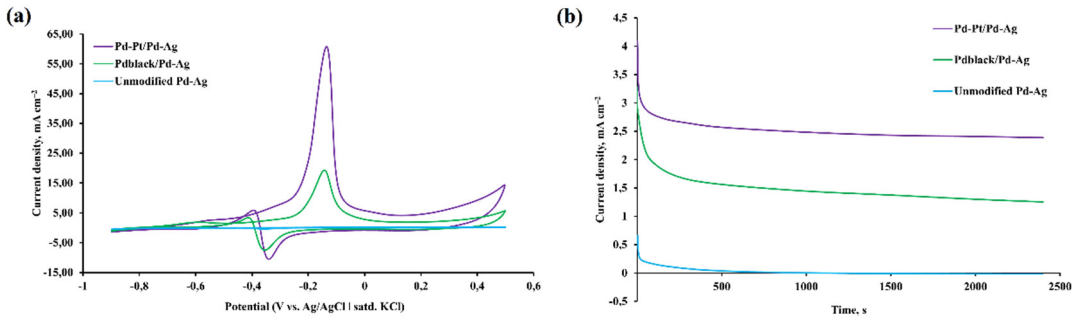

Figure 4. (a) Cyclic voltammetry curves of synthesized monometallic and bimetallic modifiers in alkaline oxidation reaction of methanol. (b) Chronoamperometric curves of synthesized monometallic and bimetallic modifiers in alkaline oxidation reaction of methanol.

Thus, bimetallic pentagonally structured Pd-Pt/Pd-Ag modifier, synthesized in this work, demonstrated excellent catalytic activity, long-term stability, and resistance to CO_{ads} poisoning in alkaline oxidation reaction of methanol. The achieved results can be due to both the synergistic effect of the combination of palladium and platinum metals and the large number of available catalytically active centers, which are results of the non-classic morphology with high-index facets.

2.3. Diffusion and selective characteristics of bimetallic Pd-Pt modifier on pentatwinned nanoparticles basis

Developed bimetallic pentagonally structured Pd-Pt/Pd-Ag modifier was studied in hydrogen transport processes to assess gas transport characteristics. Resulting characteristics were compared with those of classic Pd_{black}/Pd-Ag modifier and unmodified membrane. In the first series of experiments, diffusion characteristics of obtained membranes were assessed in terms of hydrogen permeate flux density as a function of temperature in the range from 25 to 100 °C and pressure 0.4 MPa. The choice of this temperature range is based on the role and properties of the modifier to achieve permeability for palladium-based membranes even at room temperature. Figure 5a shows the temperature dependence of hydrogen flux density for membranes with pentagonally structured modifier and classic one. Data for the smooth unmodified Pd-Ag membrane are shown for comparison. It is evident, that the flux of hydrogen permeating through the membranes increases with the rise of permeation temperature. However, it should be noted that the permeation flux was not recorded up to a temperature of 50 °C for unmodified membrane, while modified membranes showed hydrogen permeation flux density up to 14.7 mmol s^{-1} m^{-2} for Pd-Pt/Pd-Ag and 10.1 mmol s^{-1} m^{-2} for Pd_{black}/Pd-Ag already at a temperature of 25 °C. The highest values of hydrogen permeation flux density at 100 °C were demonstrated by the membrane with pentagonally structured Pd-Pt/Pd-Ag modifier - up to 27.3 mmol s^{-1} m^{-2}. Obtained hydrogen flux density was 2 times higher than that for membranes with classic Pd_{black}/Pd-Ag modifier, up to 13 mmol s^{-1} m^{-2}, and an order of magnitude higher than that for unmodified membrane. To confirm the hypothesis of the influence of surface processes on permeability in the selected low-temperature range, activation energy (E_A) was calculated using the Arrhenius equation [65]:

$$P_{H_2} = P_0 \exp\left(\frac{-E_A}{RT}\right) \quad (4)$$

where P_{H_2} – hydrogen permeability, P_0 – pre-exponential multiplier , R – universal gas constant, T – temperature. It is known from the literature [66], that E_A values below 30 kJ mol^{-1} indicate a significant contribution of diffusion to the hydrogen transfer process, while surface phenomena require much higher activation energy up to 146 kJ mol^{-1}. The E_A for developed membranes was estimated to be about 75 kJ mol^{-1} for unmodified membrane and about 49 kJ mol^{-1} for the membrane with pentagonally structured Pd-Pt/Pd-Ag modifier. Such results can be caused not only by activation of the membrane surface, which accelerates surface limiting processes in the range of low temperatures (up to 100 °C), but also by special morphology and structure of nanoparticles in the composition of pentagonally structured modifier. Pentagonally structured particles, in contrast to classic spherical particles, have a large number of available catalytically active centers due to the

Preprints (www.preprints.org) | NOT PEER-REVIEWED | Posted: 21 November 2023 doi:10.20944/preprints202311.1260.v1

presence of high-index high-energy facets. The synergetic effect of the favorable combination of palladium and platinum metals in the modifier also makes a significant contribution. These conclusions are confirmed by electrochemical studies presented earlier, the results of which correlate closely with those of the gas transportation studies.

The second series of experiments was carried out to support obtained data on the effect of developed modifiers on hydrogen permeability of palladium-containing membranes. During these experiments, the dependence of permeate flux density as a function of overpressure in the range from 0.05 to 0.4 MPa and temperature 25 °C was studied. Figure 5b shows the pressure dependence of hydrogen flux density for membranes with pentagonally structured modifier and classic one. A smooth unmodified Pd-Ag membrane is shown for comparison. In the conducted experiment, a similar dependence of penetration flux density was observed as in the previous series of experiments. Higher feed pressure determined higher driving force for hydrogen permeation, causing an increase in the density of flux permeated through the membrane. The membrane with pentagonally structured Pd-Pt/Pd-Ag modifier had the highest hydrogen permeation flux density at 0.4 MPa, up to 14.7 mmol s^{-1} m^{-2}. Achieved hydrogen flux density was 1.5 times higher than for membranes with classic Pd_{black}/Pd-Ag modifier, up to 10.1 mmol s^{-1} m^{-2}, and two order of magnitude higher than for unmodified membrane. However, the main point of this series of experiments was to identify the limiting stage of hydrogen transport for developed membrane materials. The hydrogen flux permeating through the membrane is expressed as follows [67]:

$$J_{H_2} = \frac{P_{H_2}}{\delta}(p_1^n - p_2^n) \qquad (5)$$

where J_{H_2} – penetrating hydrogen flux, P_{H_2} – hydrogen permeability, δ – membrane thickness, p_1^n and p_2^n – partial pressure on inlet and outlet sides of the membrane, respectively, n – pressure exponent. The exponent n can be from 0.5 to 1. At the boundary value n=0.5, equation (5) turns into Sieverts-Fick law and points to a limitation of the transfer process by diffusion of atomic hydrogen in the volume. In contrast, at the boundary value of n=1, equation (5) indicates that the transport process is limited by surface reactions, i.e., hydrogen dissociation/recombination takes longer time and consequently consumes more energy than diffusion. According to the data presented in Figure 5b, obtained permeate flux density for unmodified membrane is easily approximated by a first order line. The n value was 0.98, which means that the transport process is completely limited by surface stages. This is confirmed by activation energy, which was calculated above. For membranes with pentagonally structured modifier, the exponent n was about 0.76, which indicates the control of hydrogen permeation flux by a combination of several mechanisms, namely volumetric diffusion and surface processes. Moreover, it is confirmed by the evidently decreased activation energy in comparison with unmodified membrane. The conducted series of experiments confirms the acceleration of dissociative adsorption and recombinative desorption processes, which are limiting in the low-temperature range. Such acceleration was achieved by activation of the membrane surface with bimetallic pentagonally structured modifier with an increased number of reactive active centers towards hydrogen.

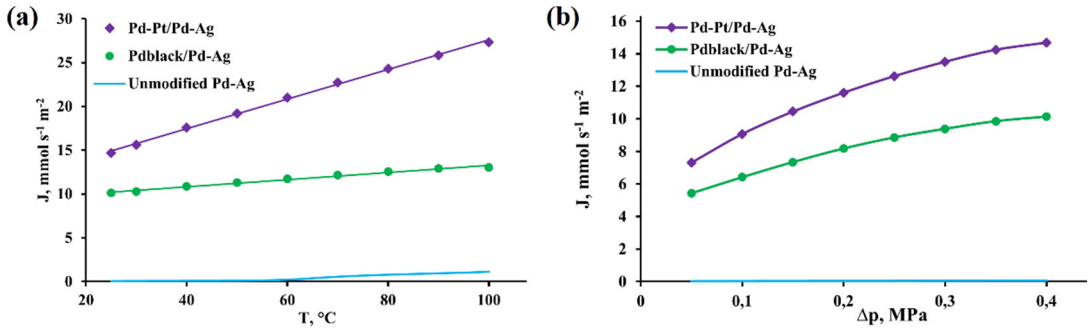

Figure 5. (a) Temperature dependence of hydrogen flux density at 0.4 MPa overpressure through membranes modified with developed monometallic and bimetallic nanoparticles. (b) Hydrogen flux density dependence on overpressure at 25 °C through membranes modified with developed monometallic and bimetallic nanoparticles.

Preprints (www.preprints.org) | NOT PEER-REVIEWED | Posted: 21 November 2023 doi:10.20944/preprints202311.1260.v1

In the third series of experiments, hydrogen permeation and nitrogen leakage tests of developed membranes with bimetallic pentagonally structured Pd-Pt/Pd-Ag modifier were performed at 25 °C and transmembrane pressure range from 0.1 to 0.4 MPa to assess selectivity. The results were compared with those for classic Pd_{black}/Pd-Ag modifier and unmodified membrane. Figure 6 shows long-term permeability data for membranes with pentagonally structured modifier and classic one for 300 hours. A smooth unmodified Pd-Ag membrane is shown for comparison. According to the results, developed membranes showed high selectivity over a long period of time. The membrane with pentagonally structured Pd-Pt/Pd-Ag modifier demonstrated the highest H_2/N_2 selectivity at a pressure of 0.4 MPa – up to 3514. Achieved selectivity was 1.2 times higher than for the membranes with classic Pd_{black}/Pd-Ag modifier, up to 3019, and was 1.5 times higher than for unmodified membrane. It can be seen from the data, that the hydrogen permeation flux was increasing with each pressure rise and stabilized over time. During the whole penetration test, there was a slight drop in selectivity in the selected pressure range (0.1–0.4 MPa), but in numerical equivalent it could be considered as insignificant. It should be noted, that the hydrogen flow was stabilized at a fixed pressure each time, and the nitrogen leakage did not increase either. This proves that developed membranes demonstrate stability and resistance to pressure drops over a long period of time, as well as the absence of significant mechanical defects such as holes and seals.

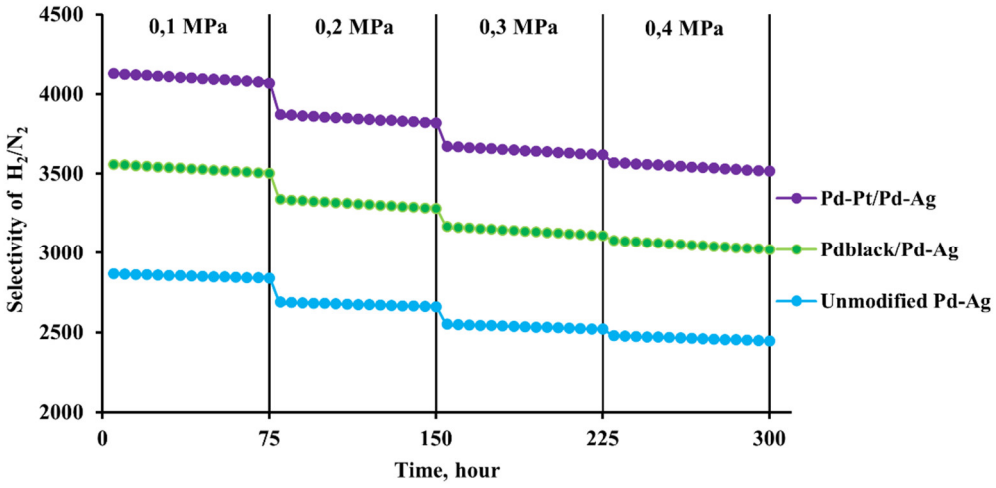

Figure 6. Selectivity dependence on overpressure at 25 °C through membranes modified with developed monometallic and bimetallic nanoparticles.

3. Materials and Methods

Creation of a membrane basis, methods of its modification and study of its surface morphology

A membrane basis is thin palladium-silver foils, which were obtained by alloying palladium and silver components in an electric arc furnace. These metals in the form of ingots were immersed in a crucible and then alloyed in a chamber under a pressure of 0.05 MPa at a varying inverter current from 12 to 120 A. The resulting Pd-23%Ag alloy ingot was rolled on DRM–130 rollers (Durston, UK) with intermediate annealings to a foil thickness of 20 μm.

The modification of obtained Pd-23%Ag foils was carried out by electrolytic deposition in galvanostatic mode on potentiostat-galvanostat P–40X (Elins, Russia) in two ways. In the first classic method for the synthesis of monometallic palladium particles, the Pd-23%Ag foil was cleaned by washing in ethanol (96 %) and degreasing in the 6 M NaOH solution. Afterwards, the prepared foil was fixed in a working electrolytic cell and polarized first anodically in 0.1 M HCl, then cathodically in 0.05 M H_2SO_4. Polarization was carried out at a current density of 10–20 mA cm^{-2}. After that, the cell was filled with the working solution of H_2PdCl_4 (2 %) for further modification. Synthesis was carried out for 1.5–5 minutes at a current density of 5–6 mA cm^{-2}. After deposition, the modified foil was washed with bidistillate.

 doi:10.20944/preprints202311.1260.v1

In the second method for the synthesis of bimetallic pentatwinned Pd-Pt nanoparticles, the Pd-23%Ag foil was also cleaned according to the procedure, which was described in the first synthesis method. Subsequently, the prepared foil was moved to a working electrolytic cell, where it was anodically and cathodically polarized in 0.1 M HCl and 0.05 M H_2SO_4, respectively. Polarization was performed at a current density of 10-20 mA cm^{-2}. Afterwards, the cell was filled with the working solution, that contained $C_{16}H_{36}BrN$ surfactant along with H_2PdCl_4 (2%). The palladium-platinum foil was used as an anode. During the synthesis process, low current density of up to 0.003 mA cm^{-2} was set for a short period of time, 30–60 s. This stage was necessary for the nucleation process. Subsequently, current density was increased to 0.25–0.3 mA cm^{-2} and particles were being grown further for 3.5–10 min. After deposition, the modified foil was washed with bidistillate.

The morphology of Pd-23%Ag modified foils was studied with electron microscopy on JSM–7500F scanning electron microscope (JEOL, Japan). The elemental composition was monitored using INCA (Oxford) semiconductor energy dispersive attachment, which is a part of JSM–7500F scanning electron microscope (JEOL, Japan).

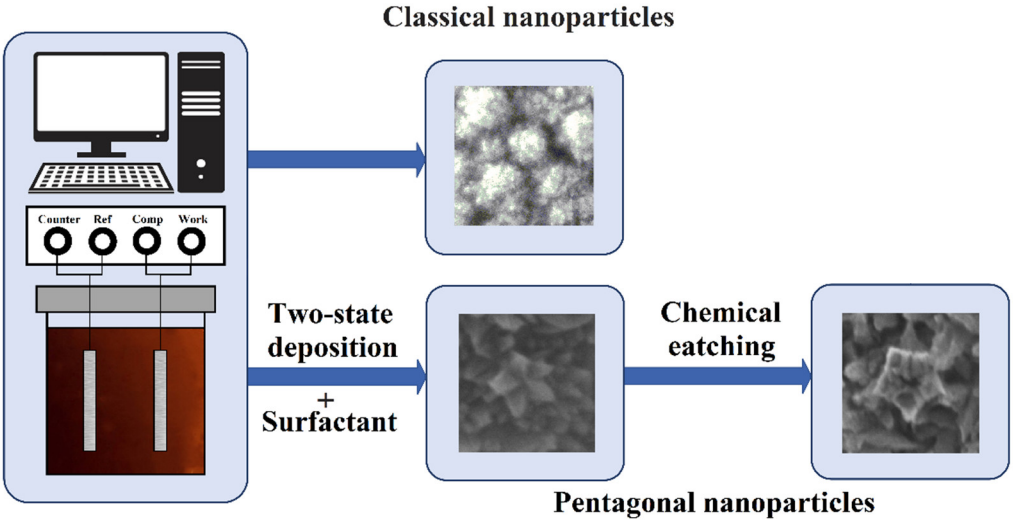

Figure 7. Schematic illustration of methods for synthesizing Pd and Pd-Pt nanoparticles.

Membrane research in catalytic and gas transportation processes

Catalytic activity of developed membrane materials was studied with cyclic voltammetry in the reaction of alkaline oxidation of methanol on potentiostat-galvanostat P-40X (Elins, Russia). The working solution consisted of 0.5 M methanol and 1M NaOH. Measurements were performed at room temperature in the potential range from – 0.9 V to + 0.5 V at a scan speed of 50 mV s^{-1}. A three-electrode cell was used for the experiments. It consisted of a working electrode, which was made of developed membrane samples, a platinum counter electrode and a glass Ag/AgCl reference electrode.

The long-term stability of the developed membrane materials was examined with chronoamperometry in the reaction of alkaline oxidation of methanol on potentiostat-galvanostat P–40X (Elins, Russia). The working solution consisted of 0.5 M methanol and 1 M NaOH. Measurements were performed at room temperature at a constant potential of – 0.3 V for 2400 s.

Gas diffusion characteristics and selectivity of developed membrane materials were tested on a hydrogen permeability measurement unit according to the methodology, which was described extensively in the paper [68]. The examined membranes were hermetically sealed with copper gaskets and mounted in the chamber. Penetration tests were performed sequentially in hydrogen at various pressures up to 0.4 MPa and temperatures from 25 to 100 °C. The hydrogen penetration rate was measured with a mass flow meter. Prior to each hydrogen penetration test, the membranes were

 doi:10.20944/preprints202311.1260.v1

first confirmed to be with no obvious defects via helium leakage tests. Selectivity was analyzed via the H_2/N_2 flux ratio.

4. Conclusions

A unique method for synthesizing a modifier based on non-classic bimetallic pentagonally structured Pd-Pt nanoparticles has been developed. This method combines classic and additional tools for adjusting shape and structure of particles, namely voltage and current. Obtained particles in the modifier composition had high-energy high-index facets. The modifier had high density of undercoordinated atoms with high reactivity. It was also found, that nanoparticles had unique hollow structure. This can significantly reduce the cost, due to the economical use of metal. According to the results of electrochemical studies, synthesized bimetallic pentagonally structured Pd-Pt/Pd-Ag modifier showed excellent catalytic activity (up to 60.72 mA cm^{-2}), long-term stability and resistance to CO_{ads} poisoning in alkaline oxidation reaction of methanol. Achieved results can be caused by both the synergistic effect of the combination of Pd and Pt metals in the modifier composition and the large number of available catalytically active centers, which are present due to the non-classic morphology with high-index facets. Very high hydrogen permeability values were recorded while analyzing the results of the membrane performance of developed materials. This became possible due to the significant facilitation of surface processes, namely dissociative adsorption and recombinative desorption for modified membranes. The membrane with pentagonally structured Pd-Pt/Pd-Ag modifier showed the highest hydrogen permeation flux density up to 27.3 mmol s^{-1} m^{-2}. Obtained hydrogen flux density was 2 times higher than that for membranes with classic Pd_{black}/Pd-Ag modifier and an order of magnitude higher than that for unmodified membrane. This result can be explained by the presence of nanoparticles in the Pd-Pt/Pd-Ag composition, which are active towards reactions involving hydrogen, due to their high-energy facets with high index. A significant increase in selectivity of developed Pd-Pt/Pd-Ag membranes was recorded – 3514, because the rate of transcrystalline hydrogen transfer through the membrane increased while the rate of transfer through defects remained unchanged. The results, which were obtained in research, are confirmed by close correlation of diffusion-selective properties in membrane hydrogen mass transfer processes with catalytic properties in processes of alkaline electrooxidation of methanol.

Author Contributions: Conceptualization, I.P.; methodology, I.P.; investigation, I.P., P.P. and G.A.; data curation, P.P. and G.A.; writing—original draft preparation, P.P. and I.P.; writing—review and editing, I.P.; visualization, G.A.; project administration, I.P.; funding acquisition, I.P. and S.D. All authors have read and agreed to the published version of the manuscript.

Funding: This research was funded by Russian Science Foundation and Kuban Scientific Foundation grant No. 22-19-20068, https://rscf.ru/project/22-19-20068/.

Institutional Review Board Statement: Not applicable.

Informed Consent Statement: Not applicable.

Data Availability Statement: The data presented in this study are available on request from the corresponding author.

Conflicts of Interest: The authors declare no conflict of interest.

References

1. Filippova, S.P.; Yaroslavtsev, A.B. Hydrogen energy: development prospects and materials. *Russ. Chem. Rev.* **2021**, *90*, 627–643. https://doi.org/10.1070/RCR5014
2. Mamun, A.; Kiari, M.; Sabantina, L. A Recent Review of Electrospun Porous Carbon Nanofiber Mats for Energy Storage and Generation Applications. *Membranes* **2023**, *13*, 830. https://doi.org/10.3390/membranes13100830
3. Perović, K.; Morović, S.; Jukić, A.; Košutić, K. Alternative to Conventional Solutions in the Development of Membranes and Hydrogen Evolution Electrocatalysts for Application in Proton Exchange Membrane Water Electrolysis: A Review. *Materials* **2023**, *16*, 6319. https://doi.org/10.3390/ma16186319
4. Migliari, L.; Micheletto, D.; Cocco, D. Performance Analysis of a Diabatic Compressed Air Energy Storage System Fueled with Green Hydrogen. *Energies* **2023**, *16*, 7023. https://doi.org/10.3390/en16207023

5. Binazadeh, M.; Mamivand, S.; Sohrabi, R.; Taghvaei, H.; Iulianelli, A. Membrane reactors for hydrogen generation: From single stage to integrated systems. *Int. J. Hydrogen Energy* **2023**, *In Press*. https://doi.org/10.1016/j.ijhydene.2023.06.266
6. Nemitallah, M.A. Characteristics of hydrogen separation and methane steam reforming in a Pd-based membrane reactor of shell and tube design. *Case Stud. Therm. Eng.* **2023**, *45*, 102939. https://doi.org/10.1016/j.csite.2023.102939
7. Aditiya, H.B.; Aziz, M. Prospect of hydrogen energy in Asia-Pacific: A perspective review on techno-socio-economy nexus. *Int. J. Hydrogen Energy* **2021**, *46*, 35027–35056. https://doi.org/10.1016/j.ijhydene.2021.08.070
8. Solomin, E.; Salah, Z.; Osintsev, K.; Aliukov, S.; Kuskarbekova, S.; Konchakov, V.; Olinichenko, A.; Karelin, A.; Tarasova, T. Ecological Hydrogen Production and Water Sterilization: An Innovative Approach to the Trigeneration of Renewable Energy Sources for Water Desalination: A Review. *Energies* **2023**, *16*, 6118. https://doi.org/10.3390/en16176118
9. Zhang, L.; Xie, G.; Liu, F.; Ji, H. High hydrogen selectivity Pd-Ni alloy film hydrogen sensor with hybrid organosilica membranes. *J. Alloys Compd.* **2023**, *941*, 168898. https://doi.org/10.1016/j.jallcom.2023.168898
10. Xu, F.; Ma, J.; Li, C.; Ma, C.; Li, J.; Guan, B.-O.; Chen, K. Fabry–Pérot Cavities with Suspended Palladium Membranes on Optical Fibers for Highly Sensitive Hydrogen Sensing. *Molecules* **2023**, *28*, 6984. https://doi.org/10.3390/molecules28196984
11. Jung, W.; Chang, D. Deep Reinforcement Learning-Based Energy Management for Liquid Hydrogen-Fueled Hybrid Electric Ship Propulsion System. *J. Mar. Sci. Eng.* **2023**, *11*, 2007. https://doi.org/10.3390/jmse11102007
12. Parra, D.; Valverde, L.; Pino, F.J.; Patel, M.K. A review on the role, cost and value of hydrogen energy systems for deep decarbonisation. Renew. *Sust. Energ. Rev.* **2019**, *101*, 279–294. https://doi.org/10.1016/j.rser.2018.11.010
13. Yin, Z.; Yang, Z.; Tong, Y.; Du, M.; Mi, J.; Yu, Q.; Li, S. Improved sulfur tolerance of Pd–Ru membranes: Influence of H2S concentration and exposure time on the hydrogen flux. *Int. J. Hydrogen Energy* **2023**, *In Press*. https://doi.org/10.1016/j.ijhydene.2023.06.102
14. Buonomenna, M.G. Proton-Conducting Ceramic Membranes for the Production of Hydrogen via Decarbonized Heat: Overview and Prospects. *Hydrogen* **2023**, *4*, 807-830. https://doi.org/10.3390/hydrogen4040050
15. Bernardo, G.; Araújo, T.; Lopes, T.S.; Sousa, J.; Mendes, A. Recent advances in membrane technologies for hydrogen purification. *Int. J. Hydrogen Energy* **2020**, *45*, 7313–7338. https://doi.org/10.1016/j.ijhydene.2019.06.162
16. Skolotneva, E.; Tsygurina, K.; Mareev, S.; Melnikova, E.; Pismenskaya, N.; Nikonenko, V. High Diffusion Permeability of Anion-Exchange Membranes for Ammonium Chloride: Experiment and Modeling. *Int. J. Mol. Sci.* **2022**, *23*, 5782. https://doi.org/10.3390/ijms23105782
17. Mareev, S.; Gorobchenko, A.; Ivanov, D.; Anokhin, D.; Nikonenko, V. Ion and Water Transport in Ion-Exchange Membranes for Power Generation Systems: Guidelines for Modeling. *Int. J. Mol. Sci.* **2023**, *24*, 34. https://doi.org/10.3390/ijms24010034
18. Zhang, K.; Way, J.D. Palladium-copper membranes for hydrogen separation. *Sep. Purif. Technol.* **2017**, *186*, 39–44. https://doi.org/10.1016/j.seppur.2017.05.039
19. Mamivand, S.; Binazadeh, M.; Sohrabi, R. Applicability of membrane reactor technology in industrial hydrogen producing reactions: Current effort and future directions. *J. Ind. Eng. Chem.* **2021**, *104*, 212–230. https://doi.org/10.1016/j.jiec.2021.08.029
20. Petriev, I.S.; Lutsenko, I.S.; Pushankina, P.D.; Frolov, V.Yu.; Glazkova, Yu.S.; Malkov, T.I.; Gladkikh, A.M.; Otkidach, M.A.; Sypalo, E.B.; Baryshev, P.M.; Shostak, N.A.; Kopytov, G.F. Hydrogen Transport through Palladium-Coated Niobium Membranes. *Russ. Phys. J.* **2022**, *65*, 312–316. https://doi.org/10.1007/s11182-022-02637-x
21. Lytkina, A.A.; Orekhova, N.V.; Ermilova, M.M.; Petriev, I.S.; Baryshev, M.G.; Yaroslavtsev, A.B. Ru–Rh based catalysts for hydrogen production via methanol steam reforming in conventional and membrane reactors. *Int. J. Hydrogen Energy* **2019**, *44*, 13310–13322. https://doi.org/10.1016/j.ijhydene.2019.03.205
22. Chen, W.-H.; Kuo, P.-C.; Lin, Y.-L. Evolutionary computation for maximizing CO2 and H2 separation in multiple-tube palladium-membrane systems. *Appl. Energy* **2019**, *235*, 299–310. https://doi.org/10.1016/j.apenergy.2018.10.106
23. Flanagan, T.B.; Oates, W.A. The Palladium-Hydrogen System. *Annu. Rev. Mater. Sci.* **1991**, *21*, 269–304. https://doi.org/10.1146/annurev.ms.21.080191.001413
24. Bosko, M.L.; Fontana, A.D.; Tarditi, A.; Cornaglia, L. Advances in hydrogen selective membranes based on palladium ternary alloys. *Int. J. Hydrogen Energy* **2021**, *46*, 15572–15594. https://doi.org/10.1016/j.ijhydene.2021.02.082
25. Zhu, K.; Li, X.; Zhang, Y.; Zhao, X.; Liu, Z.; Guo, J. Tailoring the hydrogen transport properties of highly permeable Nb51W5Ti23Ni21 alloy membrane by Pd substitution. *Int. J. Hydrogen Energy* **2022**, *47*, 6734–6744. https://doi.org/10.1016/j.ijhydene.2021.12.021

26. Alrashed, F.S.; Paglieri, S.N.; Alismail, Z.S.; Khalaf, H.; Harale, A.; Overbeek, J.P.; van Veen, H.M.; Hakeem, A.S. Steam reforming of simulated pre-reformed naphtha in a PdAu membrane reactor. *Int. J. Hydrogen Energy* **2021**, *46*, 21939–21952. https://doi.org/10.1016/j.ijhydene.2021.04.020
27. Suzuki, A.; Yukawa, H. Analysis for Reverse Temperature Dependence of Hydrogen Permeability through Pd-X (X = Y, Ho, Ni) Alloy Membranes Based on Hydrogen Chemical Potential. *Membranes* **2020**, *10*, 123. https://doi.org/10.3390/membranes10060123
28. Zhou, Q.; Luo, S.; Zhang, M.; Liao, N. Selective and efficient hydrogen separation of Pd–Au–Ag ternary alloy membrane. *Int. J. Hydrogen Energy* **2022**, *47*, 13054–13061. https://doi.org/10.1016/j.ijhydene.2022.02.044
29. Petriev, I.S.; Pushankina, P.D.; Lutsenko, I.S.; Baryshev, M.G. Anomalous Kinetic Characteristics of Hydrogen Transport through Pd–Cu Membranes Modified by Pentatwinned Flower-Shaped Palladium Nanocrystallites with High-Index Facets. *Tech. Phys. Lett.* **2021**, *47*, 803–806. https://doi.org/10.1134/S1063785021080216
30. Petriev, I.S.; Lutsenko, I.S.; Voronin, K.A.; Pushankina, P.D.; Baryshev, M.G. Hydrogen permeability of surface-modified Pd-Ag membranes at low temperatures. *IOP Conf. Ser. Mater. Sci. Eng.* **2020**, *791*, 012058. https://doi.org/10.1088/1757-899X/791/1/012058
31. Petriev, I.; Pushankina, P.; Bolotin, S.; Lutsenko, I.; Kukueva, E.; Baryshev, M. The influence of modifying nanoflower and nanostar type Pd coatings on low temperature hydrogen permeability through Pd-containing membranes. *J. Membr. Sci.* **2021**, *620*, 118894. https://doi.org/10.1016/j.memsci.2020.118894
32. Vicinanza, N.; Svenum, I.-H.; Peters, T.; Bredesen, R.; Venvik, H. New Insight to the Effects of Heat Treatment in Air on the Permeation Properties of Thin Pd77%Ag23% Membranes. *Membranes* **2018**, *8*, 92. https://doi.org/10.3390/membranes8040092
33. Petriev, I.; Pushankina, P.; Shostak, N.; Baryshev, M. Gas-Transport Characteristics of PdCu–Nb–PdCu Membranes Modified with Nanostructured Palladium Coating. *Int. J. Mol. Sci.* **2022**, *23*, 228. https://doi.org/10.3390/ijms23010228
34. Kozmai, A.; Pismenskaya, N.; Nikonenko, V. Mathematical Description of the Increase in Selectivity of an Anion-Exchange Membrane Due to Its Modification with a Perfluorosulfonated Ionomer. *Int. J. Mol. Sci.* **2022**, *23*, 2238. https://doi.org/10.3390/ijms23042238
35. Petriev, I.; Pushankina, P.; Glazkova, Y.; Andreev, G.; Baryshev, M. Investigation of the Dependence of Electrocatalytic Activity of Copper and Palladium Nanoparticles on Morphology and Shape Formation. *Coatings* **2023**, *13*, 621. https://doi.org/10.3390/coatings13030621
36. Shan, H.; Wang, W.; Wang, Z.; Ge, J.; Liu, Q.; Zhang, W.; Fu, Q. General synthesis of flexible CuO nanoparticles-anchored ZrO2 nanofibrous membranes for catalytic oxidation of tetracycline. *J. Chem. Eng.* **2023**, *466*, 143063. https://doi.org/10.1016/j.cej.2023.143063
37. Shkirskaya, S.A.; Kononenko, N.A.; Timofeev, S.V. Structural and Electrotransport Properties of Perfluorinated Sulfocationic Membranes Modified by Silica and Zirconium Hydrophosphate. *Membranes* **2022**, *12*, 979. https://doi.org/10.3390/membranes12100979
38. Basov, A.; Dzhimak, S.; Sokolov, M.; Malyshko, V.; Moiseev, A.; Butina, E.; Elkina, A.; Baryshev, M. Changes in Number and Antibacterial Activity of Silver Nanoparticles on the Surface of Suture Materials during Cyclic Freezing. *Nanomaterials* **2022**, *12*, 1164. https://doi.org/10.3390/nano12071164
39. Mutalik, C.; Saukani, M.; Khafid, M.; Krisnawati, D.I.; Widodo; Darmayanti, R.; Puspitasari, B.; Cheng, T.-M.; Kuo, T.-R. Gold-Based Nanostructures for Antibacterial Application. *Int. J. Mol. Sci.* **2023**, *24*, 10006. https://doi.org/10.3390/ijms241210006
40. Stenina, I.; Yurova, P.; Achoh, A.; Zabolotsky, V.; Wu, L.; Yaroslavtsev, A. Improvement of Selectivity of RALEX-CM Membranes via Modification by Ceria with a Functionalized Surface. *Polymers* **2023**, *15*, 647. https://doi.org/10.3390/polym15030647
41. Ramos-Zúñiga, J.; Bruna, N.; Pérez-Donoso, J.M. Toxicity Mechanisms of Copper Nanoparticles and Copper Surfaces on Bacterial Cells and Viruses. *Int. J. Mol. Sci.* **2023**, *24*, 10503. https://doi.org/10.3390/ijms241310503
42. Sogorb, M.A.; Candela, H.; Estévez, J.; Vilanova, E. Investigation of the Effects of Metallic Nanoparticles on Fertility Outcomes and Endocrine Modification of the Hypothalamic-Pituitary-Gonadal Axis. *Int. J. Mol. Sci.* **2023**, *24*, 11687. https://doi.org/10.3390/ijms241411687
43. Petriev, I.S.; Pushankina, P.D.; Lutsenko, I.S.; Baryshev, M.G. The influence of a crystallographically atypical pentagonal nanostructured coating on the limiting stage of low-temperature hydrogen transport through Pd–Cu membranes. *Dokl. Phys.* **2021**, *66*, 209–213. https://doi.org/10.1134/S1028335821080061
44. Theerthagiri, J.; Lee, S.J.; Murthy, A.P.; Madhavan, J.; Choi, M.Y. Fundamental aspects and recent advances in transition metal nitrides as electrocatalysts for hydrogen evolution reaction: A review. *Curr. Opin. Solid State Mater. Sci.* **2020**, *24*, 100805. https://doi.org/10.1016/j.cossms.2020.100805
45. Bianchini, C.; Shen, P.K. Palladium-based electrocatalysts for alcohol oxidation in half cells and in direct alcohol fuel cells. *Chem. Rev.* **2009**, *109*, 4183–4206. https://doi.org/10.1021/cr9000995

46. Alaqarbeh, M.; Adil, S.F.; Ghrear, T.; Khan, M.; Bouachrine, M.; Al-Warthan, A. Recent Progress in the Application of Palladium Nanoparticles: A Review. *Catalysts* **2023**, *13*, 1343. https://doi.org/10.3390/catal13101343
47. Sanap, K.K.; Mali, S.S.; Tyagi, D.; Shirsat, A.N.; Phapale, S.B.; Waghmode, S.B.; Varma, S. Development of a Simple Electroless Method for Depositing Metallic Pt-Pd Nanoparticles over Wire Gauge Support for Removal of Hydrogen in a Nuclear Reactor. *Materials* **2023**, *16*, 6541. https://doi.org/10.3390/ma16196541
48. Pushankina, P.; Baryshev, M.; Petriev, I. Synthesis and Study of Palladium Mono- and Bimetallic (with Ag and Pt) Nanoparticles in Catalytic and Membrane Hydrogen Processes. *Nanomaterials* **2022**, *12*, 4178. https://doi.org/10.3390/nano12234178
49. Ruditskiy, A.; Choi, S.I.; Peng, H.C.; Xia, Y. Shape-controlled metal nanocrystals for catalytic applications. *MRS Bulletin* **2014**, *39*, 727–737. https://doi.org/10.1557/mrs.2014.167
50. Liu, Q.; Rzepka, P.; Frey, H.; Tripp, J.; Beck, A.; Artiglia, L.; Ranocchiari, M.; van Bokhoven, J.A. Sintering behavior of carbon-supported Pt nanoparticles and the effect of surface overcoating. *Mater. Today Nano* **2022**, *20*, 100273. https://doi.org/10.1016/j.mtnano.2022.100273
51. Dong, K.; Dai, H.; Pu, H.; Zhang, T.; Wang, Y.; Deng, Y. Enhanced electrocatalytic activity and stability of Pd-based bimetallic icosahedral nanoparticles towards alcohol oxidation reactions. *Int. J. Hydrogen Energy* **2023**, *48*, 12288–12298. https://doi.org/10.1016/j.ijhydene.2022.12.055
52. Chen, Y.; Dai, Q.; Zhang, Q.; Huang, Y. Precisely deposited Pd on ZnO (002) facets derived from complex reduction strategy for methanol steam reforming. *Int. J. Hydrogen Energy* **2022**, *47*, 14869–14883. https://doi.org/10.1016/j.ijhydene.2022.03.003
53. Karaman, C. Engineering of N,P,S-Triple doped 3-dimensional graphene architecture: Catalyst-support for "surface-clean" Pd nanoparticles to boost the electrocatalysis of ethanol oxidation reaction. *Int. J. Hydrogen Energy* **2023**, *48*, 6691–6701. https://doi.org/10.1016/j.ijhydene.2022.02.093
54. Pushankina, P.; Andreev, G.; Petriev, I. Hydrogen Permeability of Composite Pd–Au/Pd–Cu Membranes and Methods for Their Preparation. *Membranes* **2023**, *13*, 649. https://doi.org/10.3390/membranes13070649
55. Paz-Borbón, L.O.; Johnston, R.L.; Barcaro, G.; Fortunelli, A. Structural motifs, mixing, and segregation effects in 38-atom binary clusters. *J. Chem. Phys.* **2008**, *128*, 134517. https://doi.org/10.1063/1.2897435
56. Jung, H.; King, M.E.; Personick, M.L. Strategic synergy: advances in the shape control of bimetallic nanoparticles with dilute alloyed surfaces. *Curr. Opin. Colloid Interface Sci.* **2019**, *40*, 104–117. https://doi.org/10.1016/j.cocis.2019.02.004
57. Gutkin, M.Yu.; Kolesnikova, A.L.; Yasnikov, I.S.; Vikarchuk, A.A.; Aifantis, E.C.; Romanov, A.E. Fracture of hollow multiply-twinned particles under chemical etching. *Eur. J. Mech. A/Solids* **2018**, *68*, 133–139. https://doi.org/10.1016/j.euromechsol.2017.11.004
58. Yousaf, A.B.; Khan, R.; Imran, M.; Fernandez, C.; Yuan, C.-Z.; Song, L. Synergistic Electronic Pull of Graphene Oxide Supported Pd Nanoparticles on Enhancing Catalytic Activity of Electro Deposited Pt Nanoparticles for Methanol Oxidation Reaction. *Int. J. Electrochem. Sci.* **2016**, *11*, 6735–6746. https://doi.org/10.20964/2016.08.12
59. Kim, S.-M.; Lee, Y.-J.; Kim, J.-W.; Lee, S.-Y. Facile synthesis of Pt–Pd bimetallic nanoparticles by plasma discharge in liquid and their electrocatalytic activity toward methanol oxidation in alkaline media. *Thin Solid Films* **2014**, *572*, 260–265. https://doi.org/10.1016/j.tsf.2014.07.067
60. Zhan, F.; Bian, T.; Zhao, W.; Zhang, H.; Jin, M.; Yang, D. Facile synthesis of Pd–Pt alloy concave nanocubes with high-index facets as electrocatalysts for methanol oxidation. *CrystEngComm*, **2014**, *16*, 2411–2416. https://doi.org/10.1039/C3CE42362J
61. Hanifah, M.F.R.; Jaafar, J.; Othman, M.H.D.; Ismail, A.F.; Rahman , M.A.; Yusof, N.; Aziz, F.; Rahman, N.A. One-pot synthesis of efficient reduced graphene oxide supported binary Pt-Pd alloy nanoparticles as superior electro-catalyst and its electro-catalytic performance toward methanol electro-oxidation reaction in direct methanol fuel cell. *J. Alloys Compd.* **2019**, *793*, 232–246. https://doi.org/10.1016/j.jallcom.2019.04.114
62. Woo, S.; Lee, J.; Park, S.-K.; Kim, H.; Chung, T.D.; Piao, Y. Electrochemical codeposition of Pt/graphene catalyst for improved methanol oxidation. *Curr. Appl. Phys.* **2015**, *15*, 219–225. https://doi.org/10.1016/j.cap.2014.12.022
63. Chen, D.; Zhao, Y.; Fan, Y.; Wang, W.; Li, X.; Peng, X.; Wang, X.; Tian, J. Preparation and characterization of core–shell-like PbPt nanoparticles electro-catalyst supported on graphene for methanol oxidation. *Int. J. Hydrogen Energy* **2014**, *39*, 16053-16060. https://doi.org/10.1016/j.ijhydene.2013.12.075
64. Zhang, Y.; Chang, G.; Shu, H.; Oyama, M.; Liu, X.; He, Y. Synthesis of Pt–Pd bimetallic nanoparticles anchored on graphene for highly active methanol electro-oxidation. *J. Power Sources* **2014**, *262*, 279-285. https://doi.org/10.1016/j.jpowsour.2014.03.127
65. Kim, T.-W.; Lee, E.-H.; Byun, S.; Seo, D.-W.; Hwang, H.-J.; Yoon, H.-C.; Kim, H.; Ryi, S.-K. Highly selective Pd composite membrane on porous metal support for high-purity hydrogen production through effective ammonia decomposition. *Energy* **2022**, *260*, 125209. https://doi.org/10.1016/j.energy.2022.125209

66. Iulianelli, A.; Ghasemzadeh, K.; Marelli, M.; Evangelisti, C. A supported Pd-Cu/Al2O3 membrane from solvated metal atoms for hydrogen separation/purification. *Fuel Process. Technol.* **2019**, *195*, 106141. https://doi.org/10.1016/j.fuproc.2019.106141
67. Yin, Z.; Yang, Z.; Du, M.; Mi b , J.; Hao, L.; Tong, Y.; Feng, Y.; Li, S. Effect of annealing process on the hydrogen permeation through Pd–Ru membrane. *J. Membr. Sci.* **2022**, *654*, 120572. https://doi.org/10.1016/j.memsci.2022.120572
68. Petriev, I.S.; Pushankina, P.D.; Andreev, G.A. Investigation of Low-Temperature Hydrogen Permeability of Surface Modified Pd–Cu Membranes. *Membr. Membr. Technol.* **2023**, *5*, 360–369. https://doi.org/10.1134/S2517751623050074